Macroscopic currents of ionic channels using Mass Action Law: A mathematical model

Corrientes macroscópicas de canales iónicos mediante la ley de acción de masas: Un modelo matemático

DOI: 10.46932/sfjdv2n5-086

Received in: Oct 1st, 2021
Accepted in: Dec 30th, 2021

Torres Jácome Julián
Laboratorio de Fisiopatología Cardiovascular. Benemérita Universidad Autónoma de Puebla 1152, 72000 Puebla, Puebla, México.
E-mail: jtorresjacome@gmail.com

Martagon-Domínguez Juan Mauricio
Facultad de Ciencias Físico Matemáticas Benemerita Universidad Autonoma de Puebla. Apartado postal 1152, 72000 Puebla, Puebla, México.
E-mail: jmmartagond@gmail.com

Montes Pérez Areli
Facultad de Ciencias Físico Matemáticas Benemerita Universidad Autonoma de Puebla. Apartado postal 1152, 72000 Puebla, Puebla, México.
E-mail: arelimp@fcfm.buap.mx

Montiel-Jaen Guadalupe
Departamento de Bioquímica CINVESTAV-IPN: Apartado postal 07360 ciudad de México, México.
E-mail: g.montiel04@yahoo.com.mx

García-Garibay Otto
Laboratorio de Fisiopatología Cardiovascular. Benemérita Universidad Autónoma de Puebla 1152, 72000 Puebla, Puebla, México.
E-mail: elottito@hotmail.com

Moran-Raya Carolina
Laboratorio de Aplicaciones Biotecnologicas, Centro de Investigación de Fisicoquímica de Materiales, ICUAP. Benemérita Universidad Autónoma de Puebla 1152, 72000 Puebla, Puebla, México.
E-mail: carolina.moran@correo.buap.mx

Albarado-Ibañez Alondra
Laboratorio de Aplicaciones Biotecnologicas, Centro de Investigación de Fisicoquímica de Materiales, ICUAP. Benemérita Universidad Autónoma de Puebla 1152, 72000 Puebla, Puebla, México.
E-mail: a100102@hotmail.com

ABSTRACT
In this work it proposes a mathematical model for ion channels based on two concepts, the Hodgkin and Huxley's as well as the Law of Mass Action in addition, we consider the kinetics of channels as a dynamic process of Markov`s chain. With the previous premises, a system of differential equations is proposed that when it is solved, all properties of the macroscopic currents are determined. The activation, deactivation, inactivation, and recovery of the inactivation concepts remain as processes that are part of a chemical reaction. With this system of equations, all the experimental protocols used in electrophysiology to characterize macroscopic currents can be modeled. Another advantage is that the model allows, with the same system of equations, to determine the properties of voltage-dependent channels regardless of the type of ion that pass through in the channel.

Keywords: Marcov`s Chain, differentials equation system, ionic channels, macroscopic currents, kinetic of channel.

RESUMEN
En este trabajo se propone un modelo matemático para los canales iónicos basado en dos conceptos, el de Hodgkin y el de Huxley, así como en la Ley de Acción de Masas, además se considera la cinética de los canales como un proceso dinámico de cadena de Markov. Con las premisas anteriores, se propone un sistema de ecuaciones diferenciales que al resolverlo se determinan todas las propiedades de las corrientes macroscópicas. Los conceptos de activación, desactivación, inactivación y recuperación de la inactivación quedan como procesos que forman parte de una reacción química. Con este sistema de ecuaciones se pueden modelar todos los protocolos experimentales utilizados en electrofisiología para caracterizar las corrientes macroscópicas. Otra ventaja es que el modelo permite, con el mismo sistema de ecuaciones, determinar las propiedades de los canales dependientes de voltaje independientemente del tipo de ion que pase por el canal.

Palabras clave: Cadena de Marcov, sistema de ecuaciones diferenciales, canales iónicos, corrientes macroscópicas, cinética del canal.

1 INTRODUCTION

The most important physiological mechanisms in the organisms are communication between cells, transport of molecules across cellular membranes and cellular excitability, as the function of tissues, organs and systems depend on these phenoms (Rudy & Quan, 1987). In excitable cells, ionic currents across membranes are essential since they determine the value of the resting potential, its excitability and morphology of the action potential. The current originated by all channels of membrane are known as macroscopic currents, which has several, specific and number protein of channel(Caputo, Bezanilla, & DiPolo, 1989). Any alteration in the assembly line of the ionic channels such as mutations or changes in the number of transmembrane proteins, produce that the function of the cell is affected electrophysiological on the macroscopic current consequently, all pathologies that develop by defects in the ionic channels are called channelopathies. These diseases depend on type of ion channel as congenital myasthenia syndrome that originate by alterations in sodium channel, hemiplegia migraine,

supraventricular arrhythmias. The alterations of potassium channel produce ataxia muscle, epilepsy, encephalopathy, ventricle arrhythmias and others(Sanguinetti & Tristani-Firouzi, 2006).

Ion channels can be studied in detail by biophysical techniques which include the analysis of single channel molecules by patch-clamping (Caputo, Bezanilla, & Horowicz, 1984). Electrophysiological analyses of ion channels are important insights into the pathological mechanisms of channelopathies (Amin, Asghari-Roodsari, & Tan, 2010; Feske, 2010), as the alterations of ionic channels could be structural, states of channel: open, inactivated closed and resting closed. The gating opening and closing of ion channels controller diverse cellular factors for example in neuron and B cell release neurotransmitter and hormones respectively,(Cha, Ruben, George, Fujimoto, & Bezanilla, 1999). For this reason, theoretical models of transmembrane transport play a critical role in developing our understanding of the function, the mechanisms underlying electrical signaling and cellular excitability also some of it associated to different pathologies (Cha, Snyder, Selvin, & Bezanilla, 1999). The model is based in the mass-action law(Catterall, Wisedchaisri, & Zheng, 2017), we were proposed to originate differential equations to demonstrated that the gating of ion channel is like to a chemical reaction (Castillo et al., 2015). The gating, opening, and closing of ion channels is controlled by diverse factors, such as membrane potential (voltage), ligands (e.g., hormones and neurotransmitters), second messengers (e.g., calcium and cyclic nucleotides), light, temperature, and mechanical changes(Cha, Ruben, et al., 1999). In this paper we will begin by considering that the kinetics of the channels depends on the voltage. With this assumption, we generate the following model in based the previous concept and the following the concepts Hodgkin and Huxley's as well as in the Law of Mass Action.

2. METHODS

2.1THE MODEL

Since 1950, the dynamics of cell membrane potential is explained by that the changes in conductance in the cell membranes are produced by the opening of the voltage-dependent ion channels present in them(Rudy, 2009). Voltage-gated channels typically exist in one of the three states: open, inactivated closed (refractory period), and resting closed(Rudy, 2007). The channels may transit from one state to another in each voltage as a function of time that is named channel kinetic and is determined by the transition speeds between its states. The process of change closed to the open state (C-O) is known activation, the transition between the open to the closed state (O-C) is called deactivation to the transition from the open to the inactive state (O-I), is called inactivation and the transition from the inactivated state to the open (I-O) is called recovery from inactivation, and it is important to note, only state of the channel that allows the passage of current is the open state of the channel (O)(Rudy, 2007). In the assumption that

all channels of the same type have similar conductance, the percentage of channels in the open state (O) will give us the membrane conductance associated with this channel(Rudy, 2009).

It is proposed that the kinetics of a channel is a dynamic process, to placing the membrane to the voltage of channel activation, these pass from the activated state to the inactivated and recover from inactivation and off all the time(Rudy, 2008). Then the channels in the membrane reach a steady state characterized in that the percentage of channels in each of the possible states does not change, without this meaning that a channel remains in a single state at a voltage. The percentage of channels in the steady state is defined by the values of transition rates between different states. For this work we assume that the transition speeds dependent only voltage and time.

To generating the model uses the following assumptions:

1. The total number of channels in the cell membrane is constant
2. The ion channels have three closed states one open and one inactive, the passage between these states AS a Markov´s-type (Andreozzi, Carannante, D'Addio, Cesarelli, & Balbi, 2019)chemical reaction (reaction 1).
3. The passage of states is governed by the law of mass action.
4. Transition rates are functions of voltage and time, i.e. αi=αi(v,t), βi=βi(v,t), γ=γ(v,t) and δ=δ(v,t) (see reaction 1). In addition, the Ci, O and I (channel concentrations in each state) are functions of time at each value of αi, of βi γ and δ. The voltage dependence of the velocities is as reported in the literature.
5. The only conductive state is the open state O(t).

Reaction 1 $$C_1 \underset{\beta_1(V,t)}{\overset{\propto_1(V,t)}{\rightleftarrows}} C_2 \underset{\beta_2(V,t)}{\overset{\propto_2(V,t)}{\rightleftarrows}} C_3 \underset{\beta_3(V,t)}{\overset{\propto_3(V,t)}{\rightleftarrows}} O \underset{\delta(V,t)}{\overset{\gamma(V,t)}{\rightleftarrows}} I$$

For simplicity, we will only consider that the channel has 3 closed states, one open and one inactive. If there were more closed, open, or inactive states, they would only have to be put in the reaction and the system of differential equations to be solved would be determined.

Using the law of mass action(Trachtman, 2006) in reaction 1, the following system of differential equations is obtained.

(1) $\frac{dC_1(t)}{dt} = -\alpha_1 C_1(t) + \beta_1 C_2(t)$

(2) $\frac{dC_2(t)}{dt} = \alpha_1 C_1(t) - \beta_1 C_2(t) - \alpha_2 C_2(t) + \beta_2 C_3(t)$

(3) $\frac{dC_3(t)}{dt} = \alpha_2 C_2(t) - \beta_2 C_3(t) - \alpha_3 C_3(t) + \beta_3 O(t)$

(4) $\frac{dO(t)}{dt} = \alpha_3 C_3(t) - \beta_3 O(t) - \gamma O(t) + \delta I(t)$

(5) $\frac{dI(t)}{dt} = \gamma O(t) - \delta I(t)$

The equation 1 is explained because the concentration of C1 decreases when the channels of C1 pass to the C2 state with speed α1 and increases when the channels of the C2 state pass to the C1 state with speed β1.

For the solution of the equation's system, it considers that all the channels are in C_1 state and the sum of all the channels will be 1, namely the initials conditions are C1(0) = 1, C2(0) = C3(0) = O (0) = I (0) = 0, in additions to $\alpha_1 = \alpha_2 = \alpha_3 = \alpha$, and, that $\beta_1 = \beta_2 = \beta_3 = \beta$. With this condition the value of O(t) only can be between 0 and 1 and O(t)*100 gives the percentage of channels in this state at time t. In this model using the law of conservation of mass we obtain:

$$C1(t)+C2(t)+C3(t)+O(t)+I(t)=1 \text{ for all } t$$

The system of equations can be view:

$$\begin{pmatrix} C_1' \\ C_2' \\ C_3' \\ O' \\ I' \end{pmatrix} = \begin{pmatrix} -\alpha(V)C_1 + \beta(V)C_2 \\ \alpha(V)C_1 - \beta(V)C_2 - \alpha(V)C_2 + \beta(V)C_3 \\ \alpha(V)C_2 - \beta(V)C_3 - \alpha(V)C_3 + \beta(V)O \\ \alpha(V)C_3 - \beta(V)O - \gamma(V)O + \delta(V)I \\ -\delta(V)I + \gamma(V)O \end{pmatrix}$$

$$\begin{pmatrix} -\alpha(V) & \beta(V) & 0 & 0 & 0 \\ \alpha(V) & -(\alpha(V)+\beta(V)) & \beta(V) & 0 & 0 \\ 0 & \alpha(V) & -(\alpha(V)+\beta(V)) & \beta(V) & 0 \\ 0 & 0 & \alpha(V) & -(\beta(V)+\gamma(V) & \delta(V) \\ 0 & 0 & 0 & \gamma(V) & -\delta(V) \end{pmatrix} \begin{pmatrix} C_1 \\ C_2 \\ C_3 \\ O \\ I \end{pmatrix}$$

Defining the A matrix and using the Gauss-Jordan method to obtain the diagonal matrix

$$\sim \begin{pmatrix} -\alpha(V) & \beta(V) & 0 & 0 & 0 \\ 0 & -\alpha(V) & \beta(V) & 0 & 0 \\ 0 & 0 & -\alpha(V) & \beta(V) & 0 \\ 0 & 0 & 0 & -\gamma(V) & \delta(V) \\ 0 & 0 & 0 & 0 & 0 \end{pmatrix}$$

The eigenvalues of the characteristic polynomial were calculated

$$det\,(A-\lambda I) = (-\alpha(V)-\lambda)(-\alpha(V)-\lambda)(-\alpha(V)-\lambda)(-\gamma(V)-\lambda)(-\lambda) = 0$$

giving 3 equal eigenvalues and one zero, so it was decided to solve numerically the system of equations. Consequently, if we solve this system of equations considering a value for the transition velocities at a voltage Vp and plot O=O (t, Vp), we will have the normalized conductance of the current as a function of time for each voltage. In other words, the next function O (t, Vp) represents open channels percentage which the electrical current through. The solution of the system of differential equations will be done numerically using the software Mathematica®.

And the current at voltage will be calculated as

$$\text{Equation 6} \qquad i = G_{ion} O(t)[V_m - V_{ion}]$$

Where G_{ion} is the highest conductance of the corresponding ion, O(t) is the conductance function normalized to the voltage V_m (membrane voltage) and V_{ion} is the ion equilibrium potential(Stein & Walley, 1983).

2.2 PROTOCOL MODELING

To determine, its time course of the current in each voltage, the protocols used in voltage-clamp experimental are simulated. These consist of maintaining the cell a voltage where there is no current, this is known as maintenance voltage V_i (the channels are closed) and then suddenly changing the voltage where the channels passing from closed to open states, this is called test voltage (V) and after for a determinate time the voltage is returned to the original value (Vica). The protocols will be determined depending on the current to be modeled. In general, the following considerations are made:

1.-The total number of channels in the cell membrane is constant.

2.- All channels at the start (t=0) are in the closed state C_1.

3.- The protocols was started with values of αi= αi(v,t), βi=βi(v,t), γ=γ(v,t) and δ=δ(v,t). are zero in V_i. That is, during the maintenance potential the conductance is zero, the time interval of this condition is from t0 to t1 sec.

4.- The Fixing voltage is modeled with the values of αi= αi(v,t), βi=βi(v,t), γ=γ(v,t) and δ=δ(v,t). Determined to the voltage V (test voltage) we want to fix also the reported in the literature (experimentally). During the time interval t1 to t2

5.- The end of the pulse is modelled with the values of the αi = αi(v, t), βi = βi(v, t), γ = γ(v, t) and δ =δ (v, t), equal to the corresponding value in V_{ica}. The current of this stage of the protocol is known as tail current. Figure 1.

That is, to determine the O(t) with the voltage V fixing protocol, the system of equations is solved 3 times. First time, in the time interval (0, t1) another in the time interval (t1, t2) and the last one from t2 to t3. To each interval correspond their values of the alphas and betas, depending on the test voltage. The final conditions of each solution interval are the initial conditions for the solution of the system of equations of the following interval. In this paper, we use Mathematica9 for numerical solution of differential equation systems. By determining the maximum O(t) in the interval (t1, t2), we calculate the current by equation 6 and can obtain the current-versus-voltage curve as well as the voltage-dependent activation curve. If we measure the tail current and the inactivation curve of the channel can be determined depending on the voltage at which we measure the tail current.

Also, possible to propose protocols like the double pulse protocol simply designing the changing the time between the test pulse (P2) and the basic pulse (P1) see Figure 2, used to recovery from inactivation of complex currents like the HERG channels (Sanguinetti et al., 2005).

3 RESULTS

3.1 NON-INACTIVE CURRENT.

There is a potassium channel only has activation and deactivation, the system of equations associated to this channel (1) where the $\gamma(V, t)$ and $\delta(V, t)$ are zero, in addition we consider that $\alpha i(V, t)$ and $\beta i(V, t)$ are equal in each voltage step. And the values of the $\alpha i(V, t)$ and $\beta i(V,t)$ as a function of the voltage are respectively obtained from Hodgkin and Huxley(Hodgkin & Huxley, 1952b). The graph O(t) represents the channel conductance, note that O (0)=0 and its increase presents a delay, as reported by Hodgkin and Huxley, see Fig.3a. To obtain this delay, it is not required to raise to the fourth power the solution as Hodgkin and Huxley do, since the assumption that there are 3 closed states in the system of equations models this condition. This example shows that the steady state value of the conductance changes just by changing the value of the transition velocities in Figure 3b, the stay state value is close to hundred while in Figure 3a, is 75 only changing beta value from 0.043 to 0.43, in both graphs the alpha value is 1.9.

3.2 Potassium current model (Ik)

The potassium current reported by Hodgkin and Huxley1952 will be simulated using the values of alpha and betas reported by them, and protocols will be generated to obtain the system of differential equations corresponding to this macroscopic current. The protocol for potassium current is follows:

First, the maintenance voltage is -80 mV followed by a proof voltage V from -60 mV to 60 mV, in 10 mV steps with a 40ms of duration in each step then, return to the maintenance potential -80mV. That is, the protocol of Figure 1 is solved several times because of V changes.

For this channel using the general model where solve the system of equations (1) for each proof voltage V using SKa and Skd speeds we find the traces of O(t) to voltages from -60 to 60 see Figure 4, the conductance curve families by the model are like those reported in the article of Hodgkin and Huxley (Hodgkin & Huxley, 1952a).

$$SKa - - - - \propto (v) = \frac{0.01 * (-70 - v)}{Exp^{\frac{-70-v}{10}} - 1}$$

$$SKd - - - - \beta(v) = 0.125 * Exp^{\frac{-v-80}{80}}$$

The current versus voltage graph was constructed in the steady state using the conductance of the channel at each voltage value see Figure 4, each result was multiplied by the maximum conductance of 20.7 mS/cm2 to obtain of Figure 5.

3.3 INACTIVATION CURRENTS MODEL

If the values of the α=1.9 and β=0.43 was keep, see Figure 6a, but the changes the values γ=0.7310 and δ=0.009473, this way the channels showed your inactivation and recover from inactivation see Figure 6b. In these conditions the plot of conductance is transient, and the maximum value of the conductance O(t) is lower than when the channel is not inactive, this phenomenon is known as rectification. It is common to suppose that only when the graph of the conductance is transient the inactive channel, however let us suppose that the speed of inactivation is 3 and that of recovery from inactivation is 1.9 Figure 6c, we see that the graph of the conductance is like that Figure 6a was observe it is not transient, but it presents rectification.

3.4 THE SODIUM CURRENT MODEL (INA)

The protocol starts from the maintenance voltage at -80 mV follow by test voltage V from -100 mV to 60 mV in steps of 10mV for a time of 25 ms and then return to 40 mV this last step time 25 to 50 ms to determine the inactivation curve at steady state.

The alpha and beta equations using for the protocol are following:

$$SNaa - - - - \propto (V) = \frac{0.1(V+25)}{e^{\frac{V+25}{10}} - 1}$$

$$SNad - - - - - - \beta(V) = 4 * e^{\frac{V}{18}}$$

$$SNai - - - - - - \gamma(V) = \frac{1}{e^{\frac{V+30}{10}} + 1}$$

$$SNari - - - - - \delta(V) = 0.07 * e^{\frac{V}{20}}$$

The conductance O(t) versus time graphs is obtained solving the system of equations using the transition velocity values SNaa, SNad, SNai and Snari before described. The conductance curves are transient because this channel has inactivation. The solution gives graphs that reproduce the data like the Hodgkin and Huxley 1952 Figure 7. The same way, the current versus voltage graph was constructed with the maximum conductance of each trace multiplied by 40.3 mS/cm2 this is the maximum conductance of the channel reported by Hodgkin and Huxley in 1952 the results showed at the Figure 8.

The inactivation curve of the sodium current was constructed in the following protocol the maintenance voltage of -80mV then a test voltage from -100mV to 190mV and returning to a voltage of 40mV. The system of equations is solved using transition speeds SNaa, SNad, SNai and SNari corresponding to each voltage as shown in Figure 7 time 25 to 50 ms. In the Figure 9 shows the inactivation in the steady state of the maximum current at the voltage Vica also known as the tail current.The graph of the recovery of the inactivation of the sodium current was obtained in the following protocol, the first pulse named basic pulse starting with voltage of maintenance of -80 mV then a voltage of test of 40 mV with duration of 20 ms followed by a voltage of return of -80 mV is applied finalizing the pulse. Then, the test pulse starting with the same voltages only with difference between these pulses is variable from 2 ms to 60 ms, see Figure10a. This protocol shows the inactivation recovery graph which was constructed with the maximum value of O(t) of the test pulse between the maximum value of O(t) of the basic pulse in function of the interval of time between the application of the pulses see the Figure 10b. Finally, in the graph, the inactivation recovery was characterized by adjusting the exponential function of the latter graph.

3.5 TRANSIENT POTASSIUM CURRENT ITO

For the potassium current with inactivation, the alpha and beta identified in the protocol for the potassium output transient current Ito were used in the equations, experimental data were taken from Sun, X., et al.,(Sun, Hu, & Zhang, 2001). The maintenance voltage was -80mV, then voltage pulses of -30mV

to 50mV were applied every 10mV for 200ms, the pulse returned to a voltage of -80mV. The system of equations is solved with the transition speeds corresponding to Ito: SKtoa, SKtod, SKtoi and SKtori. O(t) is calculated and when the graphs are obtained, they reproduce the traces reported (Zheng et al., 2005) see the Figure 11.

$$SKtoa - - - - - - - - - \alpha(t) = \frac{4}{1 + e^{\frac{V-35}{-20}}}$$

$$SKtod - - - - - - - - - \beta(t) = \frac{3.5}{1 + e^{\frac{V+100}{29.5}}}$$

$$SKtoi - - - - - - - - - - \delta(t) = \frac{0.016}{1 + e^{\frac{V+19}{-9}}}$$

$$SKtori - - - - - - - - - - \gamma(t) = \frac{0.095}{1 + e^{\frac{V+19}{-9}}}$$

To determine the Ito current versus voltage curve, the maximum value of the behavior at each voltage is taken multiplied by the maximum macroscopic current conductance reported in Sun et al., plotted against the test voltage. The result of the model is shown in Figure 12, note that it is identical to the one determined experimentally under control conditions (Zheng et al., 2005). To have the model the inactivation of this current, a holding voltage of -80 mV was applied in the protocol, then the test voltage of -60 to 50 mV every 10 mV for 125 ms, following a return voltage to 40 mV (Vica) for a time of 125 ms tail current how shows Figure 11. The inactivation graph is shown in Figure 13a. The maximum value of the conductance at the voltage Vica is plotted against the test voltage V. The activation graph is constructed using the conductance of the voltage/current curve with the following equation $g(V) = \frac{I(V)}{V - V_{eq}}$

Where V, test voltage; Veq, equilibrium voltage of the potassium ion. The activation graph showed a sigmoidal line can be adjusted to a Boltzmann equation as experimental conditions, see Figure 13b.

For the recovery from the inactivation of this potassium channel, we use the protocol described for the sodium current, only the duration of the test pulse and the basic pulse changes to 125 ms and the time interval between the basic pulse and the test pulse goes from 50 to 1000 ms the O(t) graph is shown in Figure 14a. The maximum conductance of the test pulse is divided by the maximum conductance of the basic pulse, is plotted as a function of the time applied between the basic and test pulses. The inactivation recovery curve is shown in Figure 14b.

3.6 POTASSIUM RECTIFIER CURRENT IKR MODEL

The hERG channels produce the "fast delayed rectifier potassium current", IKr (Sanchez-Chapula & Sanguinetti, 2000). For the simulation, the curve activation of these currents was applied the following protocol, the maintenance voltage was -80 mV then test pulse from a voltage of -70 to 70 mV every 10mV with duration of 5000ms, finally the pulse returned to voltage to 20 mV. The transition speed values SIkra, SIkrd, Sikri and Sikrri were obtained of Youm and cols (Youm, Earm, & Ho, 2004) are:

$$SIkra - - - - - \alpha(V) = 0.00425e^{\frac{V-23.3}{11.9}}$$

$$SIkrd - - - - - - \beta(V) = 0.00002e^{\frac{V+23.6}{-15.4}}$$

$$SIkri - - - - - - - - - - \delta(V) = 0.087e^{\frac{V-23.6}{-100}}$$

$$SIkrri - - - - - - \gamma(V) = 0.033e^{\frac{V-32.7}{29.6}} + 0.015e^{\frac{V-32.7}{506.6}}$$

When the system of equations was solved with before described conditions, the results reproduce the family of O(t) curves reported by Sanchez-Chapula & Sanguinetti, 2000, see Figure 15. The current/voltage curve is plotting with measuring the maximum current in each line as a function of the test voltage, see Figure 16 (Sanguinetti & Jurkiewicz, 1990). The Kinetic of current is like reported of literature such as decreases at values greater than 10 mV test voltage is one of the currents that have a greater rectification, see Figure 16. Can also be seen in the attached data where an animation of the protocol and the generation of the current versus voltage curve is made. The activation and inactivation curves can be performed as we have done for the NA and potassium Ito currents, data not shown. The recovery of the inactivation in this current has a peculiar characteristic is faster than activation for this reason, the protocol used is known as involved tail, was originated pulse with a maintenance of voltage at -80 mv then the voltage test is applying of 10 mV with duration from 200ms to 4000 ms, finally the graph was constructed with the tail current versus each duration of the test voltage (Sanguinetti et al., 2005). When carrying out this protocol and solving the system of equations, we determine O(T) and the family of graphs we have in Figure 17.

3.7 CALCIUM CHANNEL TYPE L

Other channels voltage and ligand depend on like the calcium channel is known that this type of channel is inactive for two conditions, a change in electrical potential or by internal calcium concentration (Faber, Silva, Livshitz, & Rudy, 2007). This type of channel was studied by this model, the first assume

was that the internal calcium concentration is constant. Then, the model was added more Inactive states and assuming that it will be able to pass to some of these according to the values of the potential or the ionic concentration of calcium (Hadley & Lederer, 1991). The changes in velocities for state passage were used reported by Faber et al. and Rudy et al.(Faber et al., 2007; Rudy & Silva, 2006). For the calcium current protocol, a constant internal concentration of [Ca2+] = 6.72*10-5mM is assumed. The equilibrium potential is V=50mV. The test pulses from -90mV to 80mV every 10 mV with duration 40ms(Rudy & Silva, 2006). The system of equations to determine O(t) under these conditions was solved and the conductance curves as a function of time like those reported by Faber, et al. (Faber et al., 2007)were reproduced in the Figure 18.

4 DISCUSSION

The proposed model explains the properties of macroscopic currents as a function of the kinetics of the channels that generate them, with the advantage that the same system of equations can be used to describe all types of voltage-dependent currents regardless of ion selectivity. Note that for the solution of equations the system in this model is necessary to know the voltage-dependency of the alphas, betas, gammas, and deltas are unique for each type of channel. Consequently, if the voltage-dependency is of a sodium channel we will obtain the sodium currents, if the kinetics correspond to a calcium channel, we will model the calcium current, the same way for a voltage-dependent potassium channel. Therefore, every ion channel type has your own kinetic and is determinate to the function of transition velocities with respect to voltage. This same model can be used to determine the macroscopic currents independent of their ion selectivity. This model considers that the channels are dynamic, these channels pass through from one state to another all the time at each voltage then in the steady state the conductance constant value, is explained because the open channels pass to another non-conducting state, and they are replaced by other channels who were non-conducting state. In the steady state, the value of the conductance is determined by the transition speed values between for each voltage. The model facilitates the generation and simulation of experimental protocols to obtain the properties of macroscopic currents. The generation of experimental protocols is simple and faithful reproduction of the results reported in the literature, such as enveloped of tailing and recovery of inactivation of currents, this protocol is exceedingly difficult to model. The model explains the processes of activation, deactivation, inactivation, and recovery from inactivation as processes linked by the chemical reaction 1, presenting an idea of how the channel kinetics is carried out and with this being able to explain properties of macroscopic currents such as rectification linked to channel inactivation Figures: 6,15,16 and refractory period associated to recovery of the inactivation Figures:10,14,17. In this model the delay proposed by Hodgkin and Huxley for the activation

of the currents it is due to the number of closed states that precede the open state of the channels. The rectification concept in cardiac currents is necessary because the alterations in rectifier current and yours the I-V relationship of the time-dependent current allow prolongation of myocardial refractoriness for the wavelength diminishing sufficient the activation of channel to exceed the path length of the re-entrant circuit and originate lethal cardiac arrythmias. The currents had to rectify are exceedingly difficult to understand the channel kinetic however, this is the model to explain the rectification concept assuming that the activation speed of the channel is lower than the inactivation speed, thus decreasing the number of open channels in the steady state. In general, the speed of activation and/or inactivation make a difference between the existence of the rectifier currents. It is also explained the phenom of transient currents with activation and inactivation speed and inactivation recovery. However, if the velocities are in the same order of magnitude, there as conductance graph is not a transient as Ikr current. Using the Ohm's is studied the changes in conductance of channels, however IKr current has the inactivation speed major that activation consequently, the curve of current versus voltage is an inverted U, that is, it reaches a maximum of 10mV. The above seems to be a physical contradiction because the greater the difference in power in a circuit, the greater the current is expected, and in this case the greater the difference in voltage, the lower the current. In this work, this phenom is explaining easily with model only changes the speeds α(V, t), β(V, t) and $\gamma(V,t)$. The pharmaceutical industry invests in the knowledge of kinetic of the channels. As far as the implementation of this model in teaching will give clarity in the kinetics of the channels and the possibility that it can be explained how the drugs block the channel. Just by reviewing how the current is altered when the drug is placed, it is possible to infer in which state the channel is blocked. Also, the channelopathies could be diagnosed and found a treatment in little time as if there is a mutation in the channel that changes the time course of conductance, it can be determined what changes in the kinetics of the channel will be caused by this mutation.

On the order hand, this model in education will give students a tool that will allow them to easily imagine the kinetic of the channels. If it behaves as a reaction, it is easy to interpret whether the current increases or decreases, if one of the relapse rates changes. The implementation of for example, if the deactivation speed is increased, the maximum O(t) will be decreased, and if the deactivation speed is decreased, the maximum O(t) will be increased. In other words, if the speeds of the arrows going in the direction of the O(t) state increase, the maximum O(t) increases and if the speeds of the arrows coming out of O(t) increase the maximum decreases. In the opposite case, if the speeds of the arrows entering O(t) decrease, the maximum O(t) decreases and if the speeds of the arrows entering O(t) increase, the maximum O(t) increases. With this model, when stimulating at different frequencies the channels can participate with a different macroscopic current, while maintaining the voltage dependence of their transition speeds

constant. In the attached data (https://drive.google.com/drive/u/0/folders/1nzSqtOW9GxIpbcwNYRH9GaGMjHgmFavq) a simulation is made where Ito is stimulated at three different frequencies and the number of channels available depends on the stimulation frequency. This explains why when stimulating at different frequencies the morphologies of the action potentials are different even though the channel always has the same kinetics(Dorian & Newman, 2000; Elizalde, Barajas, Navarro-Polanco, & Sanchez-Chapula, 1999; Greene et al., 2000).

5 CONCLUSION

In the present work it is shown that to determine completely the behavior of the channels it is indispensable to determine the velocities of transition αi= αi (v, t), βi=βi (v, t), γ (v, t) and δ (v, t) since these are fundamental to totally reproduce the conductance of the channels as well as all their functional properties. The general equation system reproduced several ionic currents without the need to make "ad hoc" model for each one independent for type ion(Quintero-Perez, 2021). Although there are models use the formalism of classic thermodynamic trying to find the general expression, they need more than one equation system. In this model demonstrated that only changing the voltage dependence of the transition speeds, the currents and all your electrophysiological properties are modelling. This model presents a clear way to understand the electrical properties of the ionic channels. The advantage of this model is that allows explaining channel properties as rectification, the maximum conductance value, recovery of inactivation and other, these characteristics can be modelling only changing the transition speed between channel states. Furthermore, the implementation of the model will allow them to determinate the mechanism of diseases.

REFERENCES

Amin, A. S., Asghari-Roodsari, A., & Tan, H. L. (2010). Cardiac sodium channelopathies. *Pflugers Arch, 460*(2), 223-237. doi: 10.1007/s00424-009-0761-0

Andreozzi, E., Carannante, I., D'Addio, G., Cesarelli, M., & Balbi, P. (2019). Phenomenological models of NaV1.5. A side by side, procedural, hands-on comparison between Hodgkin-Huxley and kinetic formalisms. *Sci Rep, 9*(1), 17493. doi: 10.1038/s41598-019-53662-9

Caputo, C., Bezanilla, F., & DiPolo, R. (1989). Currents related to the sodium-calcium exchange in squid giant axon. *Biochim Biophys Acta, 986*(2), 250-256. doi: 10.1016/0005-2736(89)90474-4

Caputo, C., Bezanilla, F., & Horowicz, P. (1984). Depolarization-contraction coupling in short frog muscle fibers. A voltage clamp study. *J Gen Physiol, 84*(1), 133-154. doi: 10.1085/jgp.84.1.133

Castillo, J. P., Rui, H., Basilio, D., Das, A., Roux, B., Latorre, R., . . . Holmgren, M. (2015). Mechanism of potassium ion uptake by the Na(+)/K(+)-ATPase. *Nat Commun, 6*, 7622. doi: 10.1038/ncomms8622

Catterall, W. A., Wisedchaisri, G., & Zheng, N. (2017). The chemical basis for electrical signaling. *Nat Chem Biol, 13*(5), 455-463. doi: 10.1038/nchembio.2353

Cha, A., Ruben, P. C., George, A. L., Jr., Fujimoto, E., & Bezanilla, F. (1999). Voltage sensors in domains III and IV, but not I and II, are immobilized by Na+ channel fast inactivation. *Neuron, 22*(1), 73-87. doi: 10.1016/s0896-6273(00)80680-7

Cha, A., Snyder, G. E., Selvin, P. R., & Bezanilla, F. (1999). Atomic scale movement of the voltage-sensing region in a potassium channel measured via spectroscopy. *Nature, 402*(6763), 809-813. doi: 10.1038/45552

Dorian, P., & Newman, D. (2000). Rate dependence of the effect of antiarrhythmic drugs delaying cardiac repolarization: an overview. *Europace, 2*(4), 277-285. doi: 10.1053/eupc.2000.0114

Elizalde, A., Barajas, H., Navarro-Polanco, R., & Sanchez-Chapula, J. (1999). Frequency-dependent effects of 4-aminopyridine and almokalant on action-potential duration of adult and neonatal rabbit ventricular muscle. *J Cardiovasc Pharmacol, 33*(3), 352-359. doi: 10.1097/00005344-199903000-00002

Faber, G. M., Silva, J., Livshitz, L., & Rudy, Y. (2007). Kinetic properties of the cardiac L-type Ca2+ channel and its role in myocyte electrophysiology: a theoretical investigation. *Biophys J, 92*(5), 1522-1543. doi: 10.1529/biophysj.106.088807

Feske, S. (2010). CRAC channelopathies. *Pflugers Arch, 460*(2), 417-435. doi: 10.1007/s00424-009-0777-5

Greene, M., Newman, D., Geist, M., Paquette, M., Heng, D., & Dorian, P. (2000). Is electrical storm in ICD patients the sign of a dying heart? Outcome of patients with clusters of ventricular tachyarrhythmias. *Europace, 2*(3), 263-269. doi: 10.1053/eupc.2000.0104

Hadley, R. W., & Lederer, W. J. (1991). Ca2+ and voltage inactivate Ca2+ channels in guinea-pig ventricular myocytes through independent mechanisms. *J Physiol, 444*, 257-268. doi: 10.1113/jphysiol.1991.sp018876

Hodgkin, A. L., & Huxley, A. F. (1952a). Currents carried by sodium and potassium ions through the membrane of the giant axon of Loligo. *J Physiol, 116*(4), 449-472. doi: 10.1113/jphysiol.1952.sp004717

Hodgkin, A. L., & Huxley, A. F. (1952b). A quantitative description of membrane current and its application to conduction and excitation in nerve. *J Physiol, 117*(4), 500-544. doi: 10.1113/jphysiol.1952.sp004764

Quintero-Perez, J. R.-L. A., Reyes-Chapero Rosa Maria, Reyes-Monreal Marleni, Perez-Bonilla Maria Eugenia. (2021). Desarrollo de un simulador de la corriente funnydel nodo sinusal para la enseñanza-aprendizaje. *South Florida Journal of Development, 2*(4), 12. doi: 10.46932/sfjdv2n5-027

Rudy, Y. (2007). Modelling the molecular basis of cardiac repolarization. *Europace, 9 Suppl 6*, vi17-19. doi: 10.1093/europace/eum202

Rudy, Y. (2008). Molecular basis of cardiac action potential repolarization. *Ann N Y Acad Sci, 1123*, 113-118. doi: 10.1196/annals.1420.013

Rudy, Y. (2009). Cardiac repolarization: insights from mathematical modeling and electrocardiographic imaging (ECGI). *Heart Rhythm, 6*(11 Suppl), S49-55. doi: 10.1016/j.hrthm.2009.07.021

Rudy, Y., & Quan, W. L. (1987). A model study of the effects of the discrete cellular structure on electrical propagation in cardiac tissue. *Circ Res, 61*(6), 815-823. doi: 10.1161/01.res.61.6.815

Rudy, Y., & Silva, J. R. (2006). Computational biology in the study of cardiac ion channels and cell electrophysiology. *Q Rev Biophys, 39*(1), 57-116. doi: 10.1017/S0033583506004227

Sanchez-Chapula, J. A., & Sanguinetti, M. C. (2000). Altered gating of HERG potassium channels by cobalt and lanthanum. *Pflugers Arch, 440*(2), 264-274. doi: 10.1007/s004240000263

Sanguinetti, M. C., Chen, J., Fernandez, D., Kamiya, K., Mitcheson, J., & Sanchez-Chapula, J. A. (2005). Physicochemical basis for binding and voltage-dependent block of hERG channels by structurally diverse drugs. *Novartis Found Symp, 266*, 159-166; discussion 166-170.

Sanguinetti, M. C., & Jurkiewicz, N. K. (1990). Two components of cardiac delayed rectifier K+ current. Differential sensitivity to block by class III antiarrhythmic agents. *J Gen Physiol, 96*(1), 195-215. doi: 10.1085/jgp.96.1.195

Sanguinetti, M. C., & Tristani-Firouzi, M. (2006). hERG potassium channels and cardiac arrhythmia. *Nature, 440*(7083), 463-469. doi: 10.1038/nature04710

Stein, R. B., & Walley, M. (1983). Functional comparison of upper extremity amputees using myoelectric and conventional prostheses. *Arch Phys Med Rehabil, 64*(6), 243-248.

Sun, X., Hu, X., & Zhang, B. (2001). [Characterisation of transient outward potassium current (Ito1) in hypertrophied right ventricular myocytes from children with tetralogy of Fallot]. *Zhonghua Yi Xue Za Zhi, 81*(19), 1190-1193.

Trachtman, H. (2006). The law of mass action. *Am J Bioeth, 6*(4), 72-74; discussion W42-75. doi: 10.1080/15265160600755730

Youm, J. B., Earm, Y. E., & Ho, W. K. (2004). Modulation of HERG channel inactivation by external cations. *Eur Biophys J, 33*(4), 360-369. doi: 10.1007/s00249-003-0367-y

Zheng, H. F., Li, X. L., Jin, Z. Y., Sun, J. B., Li, Z. L., & Xu, W. X. (2005). Effects of unsaturated fatty acids on calcium-activated potassium current in gastric myocytes of guinea pigs. *World J Gastroenterol, 11*(5), 672-675. doi: 10.3748/wjg.v11.i5.672

FIGURES

Figure 1. Voltage clamping protocol. The protocol at voltage V (test voltage) is illustrated. At the time t=0 the system is held at voltage Vi (holding voltage). At time t=t1, the values of the transition velocities will be what corresponds to the voltage V (test voltage) and the system of equations is solved to obtain O(t) during the interval [t1, t2], the initial values for the solution in the interval [t2, t3] to determine the activation or inactivation curves depending on the value of Vica.

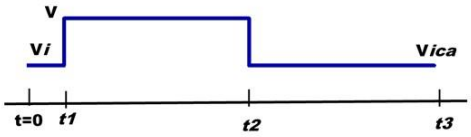

Figure 2. Double pulse protocol to determine inactivation recovery. This protocol consists of giving a square pulse at a voltage Pi (basic pulse) to generate a current, after a time interval Δt another square pulse P2 (test pulse).

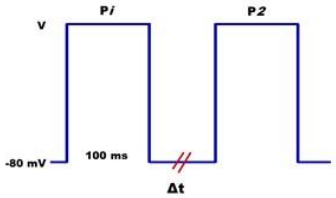

Figure 3. The conductance versus time curves described the kinetic of channels. For graph a) the values of alpha are 1.9 and the betas 0.43. For graph b) the values of alpha are 1.9 and betas 0.043. The maximum conductance shown value in the steady state is greater in graph b) than graph a) this is only if modified the value of beta.

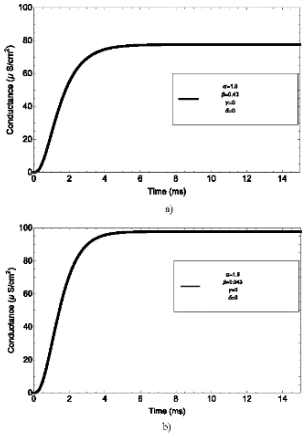

Figure 4. Model of potassium current in whole cell. The graph showed conductance with respect to time. We are using the solution of the differential equation system of the channel in open state O(t) for each voltage between -60 and 60 with 10 mV steps.

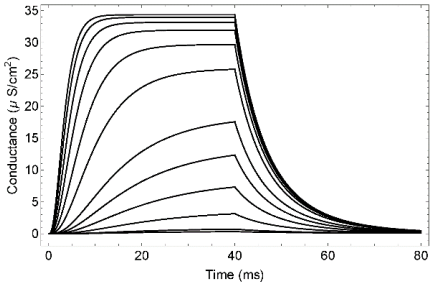

Figure 5. I versus V of potassium current. The curve showed the non-ohmic dependence of voltage in the steady state value of O(t) as reported by Hodgkin and Huxley.

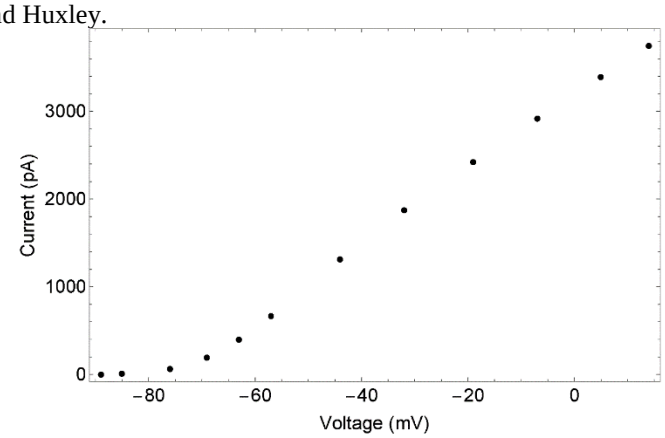

Figure 6. Conductance at a single voltage of inactivation current model. The plot a) shows the conductance of channels in the same conditions (α=1.93083, β=0.433472, γ=0, δ=0,) that Figure 3a without inactivation, b) the same voltage with inactivation (α=1.93083, β=0.433472, γ=0.731058, δ=0.00943) and c) the same voltage with faster inactivation than previous plot (α=1.93083, β=0.433472, γ=3, δ=1.9,). Note that only the γ and δ values changes.

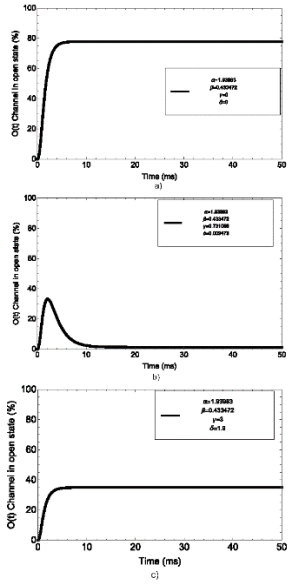

Figure 7. Conductance and Inactivation protocol in the stable state of sodium current. The graph showed conductance with respect to time O(t) obtained by the model. To a time of 25 to 50 ms, the end of the pulse is modelled with the values of the αi= αi(v, t), βi=βi(v, t),

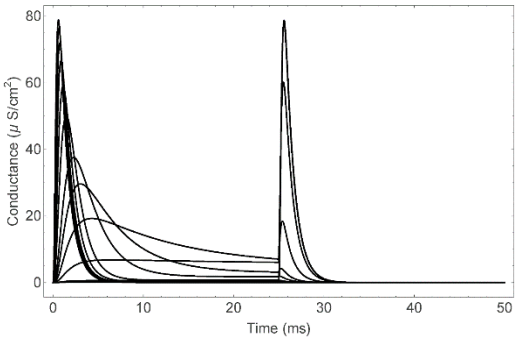

Figure 8. Current versus voltage relationship of channels sodium. For I-V plot was used, peak current amplitude in each voltage (-100 mV to 60 mV in steps of 10mV)

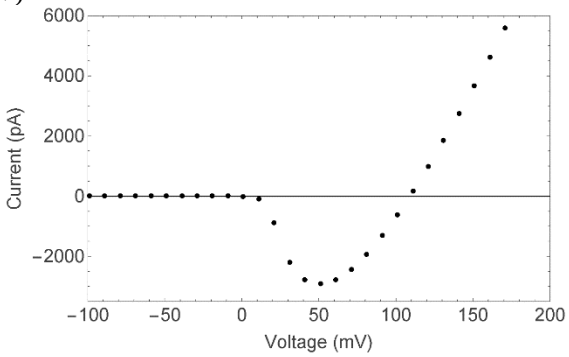

Figure 9. Inactivation curve in stable state. The conductance transients at various test voltages V are shown. The maximum of the tail current is measured (third step) to plot it as a function of the voltage of the test V, the mean amplitude at maximum values of each current component was graphed with respect to the pre-pulse potential, a similar graph is obtained as reported by Hodkin and Huxley.

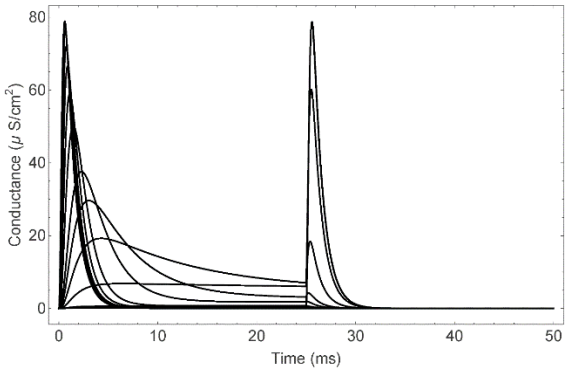

Figure 10. Recovery from the inactivation of the sodium current. In part a), the conductance traces are presented when applying the protocol of Figure 2 for the sodium channel. In section b) the maximum conductance of the test pulse is plotted divided by the maximum conductance of the basic pulse as a function of time. The graph fits a simple exponential function, and its time constant is the inactivation recovery constant

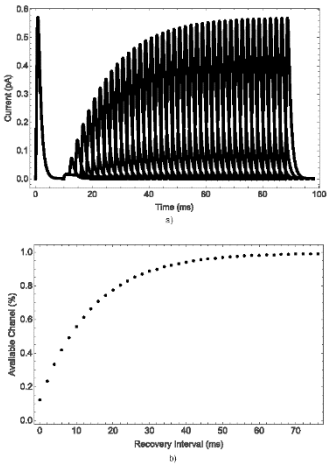

Figure 11. Conductance and inactivation of transient outward currents of potassium. The conductance graphs of the output transient potassium current Ito time [50,140] obtained by the model are shown. The traces of the tail currents in the time interval [140,250] are used to obtain the inactivation curve

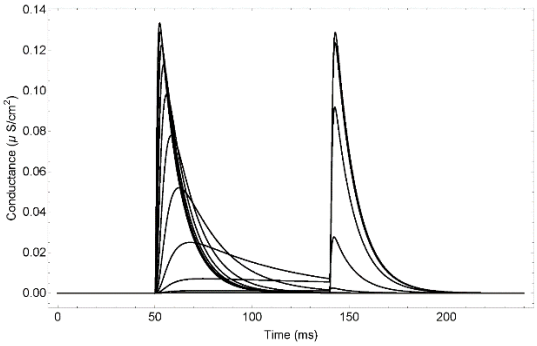

Figure 12. Current versus voltage curve of Ito. The currents versus experimental voltage curve of Ito obtained by the model are shown.

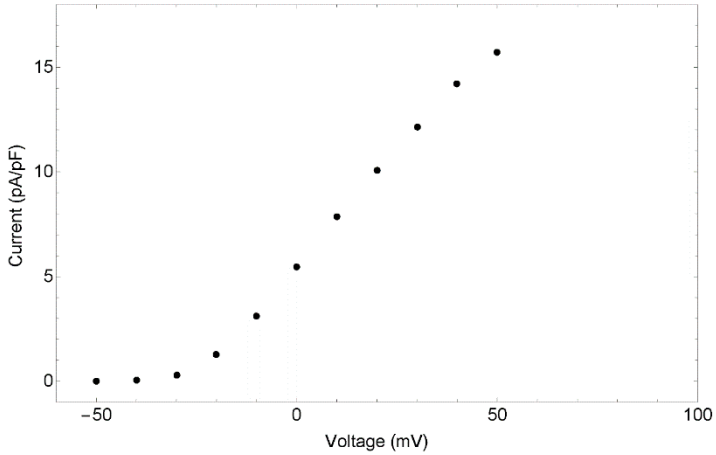

Figure 13. Inactivation and activation curves of the Ito. Shown are the inactivation curves at steady state a), and the activation curve of the Ito current generated by the model.

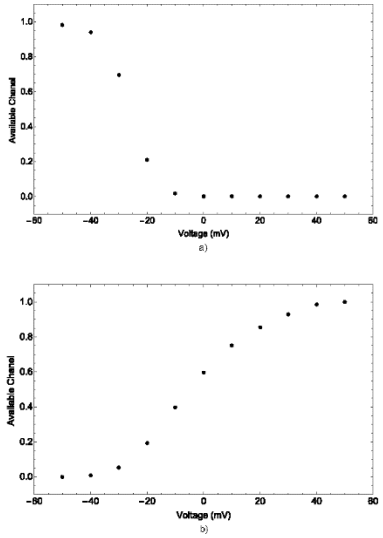

Figure 14. Recovery of the inactivation of Ito. The graphs of the model are shown when the double pulse protocol, a) is applied. b) shows the Itest /Ibasic ratio for as a function of the application time between the basic pulse and the test

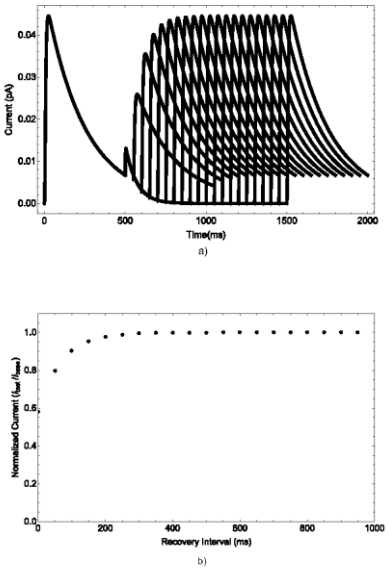

Figure 15: Conductance curves of the hERG channel produced by the model, with potential changes of 10 mV between -70 and 50 mV.

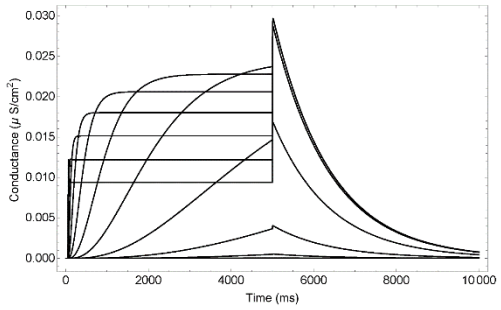

Figure 16. Ikr voltage current curve. Results of the Ikr model are presented. Note that after voting 10mV the current decreases

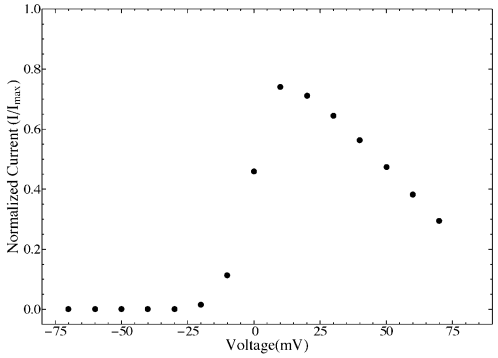

Figure 17. Tail envelope protocol. Reproduction of the duration increase experiment of the interval of test voltage V.

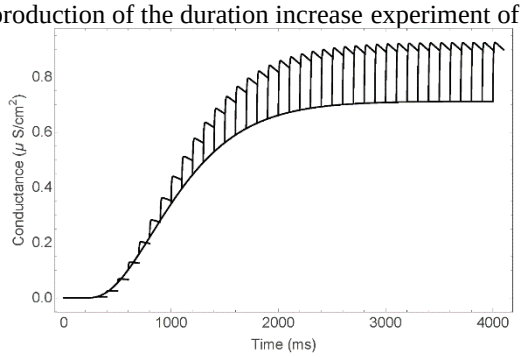

Figure 18. Calcium Current. Conductance curves of CaV channel 2:1 produced by the model, with potential changes of 10 mV between -70 and 50 mV.